



Analysis of Bit Rate and Distance Variation on Multiplexing System of Indoor Li-Fi Technology Using Movable LED Panel

Fauza Khair¹, I Wayan Mustika², Anggun Fitriani Isnawati^{3*}, Nur Azizah⁴

^{1,3,4} Institut Teknologi Telkom Purwokerto

² Universitas Gadjah Mada

³ anggun@ittelkom-pwt.ac.id

Abstract

The major problem of using light fidelity (Li-Fi) technology is still limited to the line of sight (LOS) conditions, which poses a challenge to perform bandwidth efficiency to support increased bit rates, especially for indoor use. In addition, the distance between the lamp driver (transmitter) and the receiver becomes a critical discussion to determine the characteristics of propagation losses. One solution to overcome this problem is a multiplexing system on the Li-Fi technology. Therefore, this study focuses on analyzing the performance of an indoor Li-Fi multiplexing system using a movable LED panel (LP) based on parameters of bit rate and distance variation on multiple-input multiple-output (MIMO) 2x2 and 4x4. The bit rate variations tested ranged from 10 Mbps to 40 Mbps at a distance of 3 m to 4 m. The parameter analysis of signal quality included optical and electrical signal spectrum characteristics, signal-to-noise ratio (SNR), bit error rate (BER), and Q-factor parameters. Based on the results, the increase in bit rate and distance significantly increases the BER value and decreases the Q-factor value. Both the 2x2 and 4x4 mux systems can meet standards up to a bit rate of 30 Mbps at a LOS distance of 3 meters, while at a bit rate of 40 Mbps, there are no channels that meet the ITU-T standard. In addition, the quality of the signal received at a distance of 4 meters, the 2x2 mux system can only reach the standard at a bit rate of 20 Mbps for all channels. However, channel 3 and channel 4 on the 4x4 mux system model still have the BER and Q-factor values that meet the standard in the bit rate of 30 Mbps. However, the decrease in the SNR value affected by the bit rate increase and distance is insignificant. Therefore, it becomes an opportunity for further observation of the proposed multiplexing system, detection scheme, or responsivity, and signal processing on the receiver side to be reliable on the higher bit rate.

Keywords: multiplexing; indoor Li-Fi; movable LP; bit rate

1. Introduction

The increasing use of wireless communication technology, especially the use of radio frequency (RF) spectrum, such as wireless fidelity (Wi-Fi), is getting higher [1]. Even statistical data traffic shows that the utilization of smartphones will generate more than 86% of the total mobile communication data traffic in 2021 [2]. However, along with the development of wireless communication, this RF spectrum technology faces challenges in terms of efficiency, capacity, availability, security, and the adverse effects of electromagnetic waves on human health and the environment [1]. Therefore, communication by utilizing the light spectrum is present as a solution to the limitations of RF spectrum technology, one of which is light fidelity (Li-Fi) technology [1–3].

Li-Fi is a high-speed two-way wireless communication that transfers data through the light spectrum on the downlink and the infrared spectrum on the uplink [2]

and is resistant to interference and safe for human health [4]. Li-Fi works based on the principle of visible light communication (VLC), in which data transmission is processed by modulating light waves from the visible light spectrum with a frequency 10,000 times higher than the radio frequency spectrum [5]. VLC uses visible light frequencies between 400 THz (780 nm) to 800 THz (375 nm), which can work at much higher speed data transmissions compared to the use of radio frequencies which have a frequency value below 10 GHz [6].

Li-Fi technology uses a light-emitting diode (LED) light source that is used for lighting [7] while transmitting data by creating binary codes 1 and 0 when the LED blinks, which is invisible to the human eye [8]. The utilization of LEDs as an optical source in Li-Fi technology is launched by LED panel (LP) lamp drivers using fixed, movable, and hybrid LP scenarios where each scenario provides different network coverage and

propagation systems [4]. Besides that, the most commonly used commercial LED bulbs are white LEDs and RGB (red, green, blue) LEDs that produce white light. The white LED type allows control over the color emitted and is cheaper and more efficient than the RGB method [9]. However, in VLC communication, RGB LEDs tend to be more valuable because they can control the color emitted by the light, and based on the IEEE standard for VLC describes a modulation method based on the intensity of the RGB LEDs [9].

In practical use, Li-Fi is better for indoor communication because the propagation characteristics of Li-Fi systems are still limited to line of sight (LOS) conditions [2], [8], [10]. So that if there is an external light source and the optical detector is blocked, then the signal will be disturbed even if the signal cannot be determined. Because light intensity decreases with distance from the source, the LED distance needs to be determined, and Li-Fi requires that the source and destination be in direct LOS condition [8]. Research [11] describes Li-Fi technology as the future of wireless optical communication technology, which is being widely explored. Limitations Li-Fi can only work in the LOS area so other light sources can distort the signal. However, this technology is safe for radio wave-sensitive locations such as hospitals and airplanes and prevents traffic accidents through vehicle-to-vehicle communication [12]. Therefore, multiplexing systems are used to increase the transmission range and achieve high-speed data transmission with limited modulation bandwidth [7], [13], [14]. However, in using WDM in a VLC system with several LEDs as transmitters and several photodiodes as receivers, the crosstalk between colors becomes severe as the number of wavelength divisions increases [15]. The receiver in the Li-Fi system that is commonly used is the photodiode which is a component that converts light into an electric current [14]. The photodiode involves several receiver parameters, such as the physical area of the photodiode, the field of view (FOV), and detector sensitivity. At the receiver end, a large area is used for reception using an optical concentrator to increase the effective signal reception area, provide efficient and noise-free reception amplification, and avoid using a large photodiode surface area [16].

Various models related to Li-Fi communication systems have been carried out [17]. In which indoor Li-Fi design and functionality have been developed, the use of Chebyshev filters is the best and most effective choice to increase indoor wireless connectivity because it produces high-quality and low bit error rate (BER) using the NRZ modulation scheme. The Gaussian shape of the optical pulse gives the result of a long distance and the lowest BER. At a transmission angle of 15°, the highest Q-Factor is at a low data rate of 10 Mbps, and the lower BER variations follow the lower data rate changes. In addition, various multiplexing techniques in

Li-Fi communications [14], [18] have shown that implementing a spatial multiplexing (SMX) scheme can transmit different data from each transmitter simultaneously, achieving the advantages of multiplexing but causing interference between channels (ICI) which reduces performance. Spatial modulation (SM) schemes avoid ICI, improve spectral and power efficiency, and have attracted much research [14].

Therefore, this study proposes the design of the multiplexing system on Li-Fi technology based on variations in the number of channels that are useful for bandwidth efficiency, support bit rate increases, and determine propagation losses. This study analyzes the quality of the transmission signal on two-channel and four-channel multiplexing systems with a channel spacing of 25 nm and a bit rate variation from 10 to 40 Mbps. This study also tested system performance at a distance of 3 to 4 meters (indoor use) using a movable LED panel scheme with an LED wavelength of 430 nm to 505 nm. The parameters for analyzing the quality of the received signal include signal spectrum characteristics, signal-to-noise ratio (SNR), bit error rate (BER), and Q-factor parameters.

2. Research Methods

This research proposes a model of an indoor optical wireless link multiplexing system on Li-Fi technology using movable LED panels. The system modeling is designed based on previous research models [2], [17], [19] and development on the sender and receiver sides. The indoor Li-Fi multiplexing system block generally consists of three basic blocks: the transmitter block, the indoor Li-Fi channel transmission media, and the receiver block. Modeling is devoted to implementing variations in the number of channels, namely 2 and 4 channels with multiple input multiple output (MIMO) schemes, and variations in bit rate for each channel from 10 Mbps to 40 Mbps. The overall system block is shown in Figure 1 and Figure 2.

The transmitter system block consists of a pseudo-random bit sequence generator (PRBS), which generates bit sequences according to the bit rate of the data sent, and then it is sent to the line coding process using a non-return to zero (NRZ) generator, where the results will be electrical data input which will be forwarded to the up-conversion electrical to optical (E/O) system on the transmitter side. The up-conversion mechanism in indoor Li-Fi communication is direct modulation (DM) using an optical source or optical carrier derived from an LED lamp driver. The binary bits passed through the NRZ encoding are converted by the LEDs into analog data, then are modulated into visible light. The emitted LED operates on a wavelength division multiplexing (WDM) system-ranging from a wavelength of 430 nm to 505 nm with a bandwidth of 48.64 GHz.

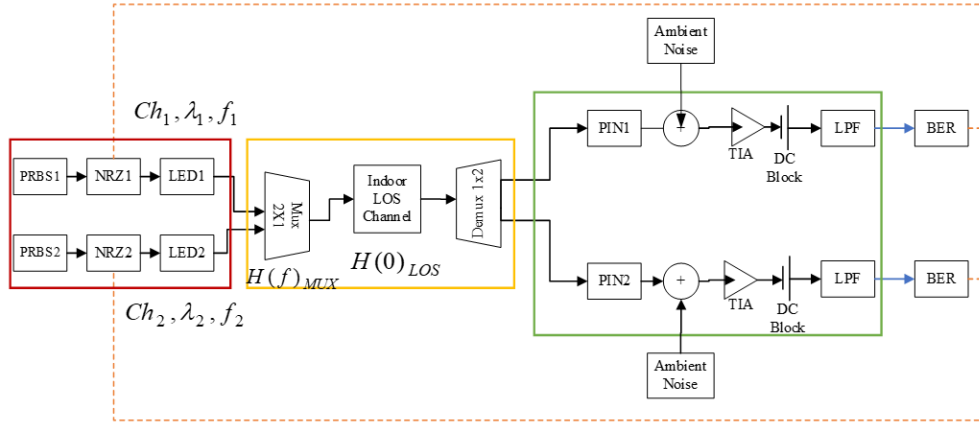


Figure 1. Diagram Block of Multiplexing 2x2 Indoor Li-Fi System

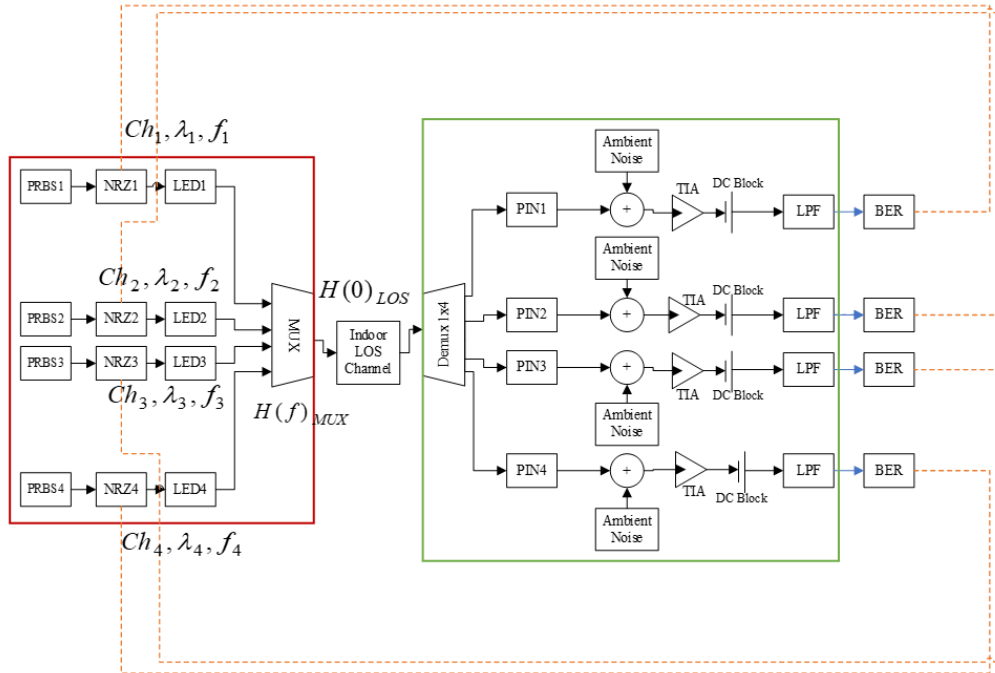


Figure 2. Diagram Block of Multiplexing 4x4 Indoor Li-Fi System

The current conversion to optical power is related to the LED's responsiveness or slope efficiency. The LED responsiveness for a single channel can be calculated based on Equation 1 [21]:

$$P = \eta \cdot h \cdot f \cdot \frac{i(t)}{q} \quad (1)$$

where η is the quantum efficiency, h is the plank constant (6.626×10^{-34} Js), f is the frequency, $i(t)$ is the modulation current signal, and q is the electron charge (1.602×10^{-19} Coulombs).

In this study, the value of the quantum efficiency for each LED used is 0.65. The characteristics of this optical modulation depend on the electron lifetime and the selected diode device, where the transfer function on the current can be formulated as Equation 2 [21]:

$$H(f)_{LED} = \frac{1}{1 + j2\pi f(\tau_n + \tau_{rc})} \quad (2)$$

where τ_n is an electron lifetime and τ_{rc} is RC constant. As for the multiplexing system modeled for 2 and 4 channels with both the 2x2 and 4x4 mux schemes which will increase bandwidth, where the formulation of total bandwidth is obtained from Equation 3 [21]:

$$B_{tot}(nm) = B_1 + B_2 + B_3 + B_4 \quad (3)$$

So that the percentage value of the quantum efficiency value is shown in Equation 4 [21]:

$$\eta_s(\%) = \left(\frac{B_{tot}}{\Delta\nu} \right) \times 100\% \quad (4)$$

where $\Delta\nu$ is the value of the channel spacing range (nm). This has an impact on the multiplexing power emitted by the LED lamp driver which refers to Equations (1) and (2), so that the power and current transfer can be formulated as Equation 5, 6, 7 and 8.

$$P_{mux} = \eta_s \cdot h \cdot f_{tot} \cdot \frac{i(t)_{tot}}{q_{tot}} \quad (5)$$

$$H(f)_{mux(2ch)} = H(f_1) + H(f_2) \quad (6)$$

$$\begin{aligned} &= \frac{1}{1 + j2\pi \cdot f_1(\tau_n + \tau_{RC})} + \frac{1}{1 + j2\pi \cdot f_2(\tau_n + \tau_{RC})} \\ H(f)_{mux(2ch)} &= \frac{1 + j2\pi \cdot f_1(\tau_n + \tau_{RC}) + 1 + j2\pi \cdot f_2(\tau_n + \tau_{RC})}{(1 + j2\pi \cdot f_1(\tau_n + \tau_{RC})) \cdot (1 + j2\pi \cdot f_2(\tau_n + \tau_{RC}))} \\ &= \frac{2 + j2\pi(f_1 + f_2)(\tau_n + \tau_{RC})}{1 + j2\pi(f_1 + f_2)(\tau_n + \tau_{RC}) - 4\pi^2 f_1^2 f_2^2 (\tau_n + \tau_{RC})^2} \\ &= \frac{2 + j2\pi(f_1 + f_2)(\tau_n + \tau_{RC})}{1 + j2\pi(f_1 + f_2)(\tau_n + \tau_{RC}) - (2\pi f_1 f_2)^2 \cdot (\tau_n + \tau_{RC})^2} \end{aligned} \quad (7)$$

$$\begin{aligned} H(f)_{mux(4ch)} &= H(f_1) + H(f_2) + H(f_1) + H(f_2) \quad (8) \\ &= \frac{1}{1 + j2\pi \cdot f_1(\tau_n + \tau_{RC})} + \frac{1}{1 + j2\pi \cdot f_2(\tau_n + \tau_{RC})} + \\ &\quad \frac{1}{1 + j2\pi \cdot f_3(\tau_n + \tau_{RC})} + \frac{1}{1 + j2\pi \cdot f_4(\tau_n + \tau_{RC})} \end{aligned}$$

Furthermore, the light emitted from a multiplexed LED is assumed to be Lambertian radiation according to the Lambertian cosine law [17]. Lambertian radian intensity is the emitted or reflected flux, which is received by per unit solid angle to per unit area [17], where the Lambertian flux intensity is obtained from the following formulation [2], [13], [17]:

$$R_0 = \left(\frac{m+1}{2\pi} \right) \cos^m \theta \quad (9)$$

$$m = - \left(\frac{\ln 2}{\ln(\cos \theta_{1/2})} \right) \quad (10)$$

where θ is the radiation angle and m is the Lambertian order obtained from Equation (10) where the variable $\theta_{1/2}$ is the value of the transmitter semi-angle at half power. Suppose it is assumed that the emission pattern of the LED lamp driver is emitting symmetrical radiation. In that case, the amount of radiation is the LED emission power multiplied by the Lambertian flux intensity. The photodetector will receive the emitted radiation with a certain acceptance angle, where the value of the power per received area W/cm^2 can refer to Equation (9) so that it can be formulated [2], [17]:

$$I_s[d, \theta] = \frac{P_t x R_0(\theta)}{d^2} \quad (11)$$

where d is the distance between the LED and the receiver. So that the amount of power received can be calculated using the value of Equation 12 [2], [17]:

$$P_r = I_s[d, \theta] \times A_{eff}(\psi) \quad (12)$$

where A_{eff} is related to the receiving structure which consists of a filter and an amplified lens, so that the area of the detector can be calculated by [17]:

$$A_{eff}(\psi) = \begin{cases} A_{det} T_s(\psi) g(\psi) \cos(\psi) & 0 \leq \psi \leq \psi_c \\ 0 & \psi > \psi_c \end{cases} \quad (13)$$

Where A_{det} is the detector area, T_s is the filter transmission gain, g is the lens gain, ψ_c is the FOV of the receiver, and ψ is the angle of incidence concerning the receiver axis. The lens gain is calculated by Equation (14) where n is the refractive index of the concentrator [17], [20]:

$$g(\psi) = \begin{cases} \frac{n^2}{\sin^2 \psi_c} & 0 \leq \psi \leq \psi_c \\ 0 & \text{otherwise} \end{cases} \quad (14)$$

By using the same considerations, the DC channel gain in the first reflection can be formulated in Equation (15) [17]. So that the value of receiving power can be found by substituting in Equation (12), and it is formulated into Equation (16) [17]:

$$\begin{aligned} H(0)_{LOS} &= \begin{cases} \frac{(m+1)A_{eff}}{2\pi d^2} \cos^m(\theta) T_s(\psi) g(\psi) \cos(\psi) & 0 \leq \psi \leq \psi_c \\ 0 & \psi > \psi_c \end{cases} \quad (15) \end{aligned}$$

$$\begin{aligned} P_r &= \begin{cases} \frac{P_t(m+1)A_{det}}{2\pi d^2 \sin^2 \psi_c \cos^m(\theta) T_s(\psi)^2 \cos(\psi)} & 0 \leq \psi \leq \psi_c \\ 0 & \psi > \psi_c \end{cases} \quad (16) \end{aligned}$$

The optical signal spectrum received by the photodetector is the result of filtering by an optical rectangle filter in anticipation of the widening of the pulse due to the emission angle, the expansion of the linewidth of the LED source, and the difference in the area of reception of the light sensor due to the increase in FOV. The system model developed from this research utilizes the DC lock placement and trans-impedance amplifier (TIA) amplification, then the amplified signal is forwarded to an electrical low pass filter (LPF). The transfer function of the filter can be formulated by [21]:

$$H(f)_{LPF} = \begin{cases} \frac{\alpha (f_c - B/2 < f < f_c + B/2)}{d} & \end{cases} \quad (17)$$

where α is the insertion loss parameter, d is the depth parameter, f_c is the filter center frequency, B is the bandwidth parameter, and f is the frequency.

This study examines and analyzes the performance of the proposed Li-Fi indoor multiplexing system by considering the transmitting parameters on the transmitter side with a transmitter half angle limit of 60° with a value of $m = 1$. In addition, tests were carried out for various LOS distances ranging from 3 m to 4 m, where the FOV value at the receiver end was 45° .

The general parameters of the proposed system model are shown in Table 1. Observation and performance analysis of the multiplexing system on indoor Li-Fi uses two scenarios of 2x2 and 4x4 mux system. LED signal emission using a movable LP scheme, then analyzed the characteristics of the transmitted optical signal spectrum. While on the receiver end, it uses a 0.2 A/W

responsive PIN photodetector, where the optical to-electrical down-conversion mechanism uses a direct detection (DD) scheme. The test results were analyzed based on the effect of variations in bit rate and distance parameters on the characteristics of the optical signal sent to the optical channel and the electrical signal after amplification and after filtering at the receiver end. System reliability is known from the quality of the received signal based on SNR, BER, and Q-factor parameters.

Table 1. General Parameter

Parameter	Mux 2 Channel	Mux 4 Channel
Wavelength	430 nm, 455 nm	430 nm, 455nm, 480 nm, 505 nm
Bit rate	10 up to 40 Mbps	10 up to 40 Mbps
Bandwidth per channel	48.64 GHz	48.64 GHz
Distance	3 up to 4 m	3 up to 4 m
Transmitter half angle	60°	60°
Index- Concentrator	1.5	1.5
FOV	45°	45°
Detector Area	1.5 cm ²	1.5 cm ²
Irradiance Angle	20°	20°
Incidence Angle	20°	20°

3. Results and Discussions

3.1 Spectral Characteristics of Optical and Electrical Signals

The optical signal spectrum from the LED output is displayed in the wavelength domain as seen from the signal peak amplitude values of each channel variation and based on the average spectrum power (dBm) of each channel using an optical spectrum analyzer (OSA). Based on the observations, an increase in the wavelength value of each transmitted channel results in a higher peak amplitude spectrum signal, as shown in Figure 3.

Furthermore, the increase of the wavelength also impacts the signal spectrum's average value, where the channel with a wavelength of 505 nm has an average power of 3.986 dBm. However, the power spectral density is narrower from the lower sideband to the upper sideband, as shown in Figure 3 (d).

On the other hand, the 430 nm channel has an average power of 1.603 dBm but has a broader power spectral, although the peak amplitude is smaller than the other channel variations, as shown in Figure 3 (a). The power spectral, which is not significantly far from the gradient values from the lower, upper and central wavelength, are shown by the 455 nm and 480 nm channels, as shown in Figures 3 (b) and 3 (c).

This result is consistent with the characteristics of the VLC signal. The different signal characteristic is caused by the modulation process but also caused by the intensity and spectral response of each channel [5].

Furthermore, the observation is focused on the electrical signal resulting from de-multiplexing and the-

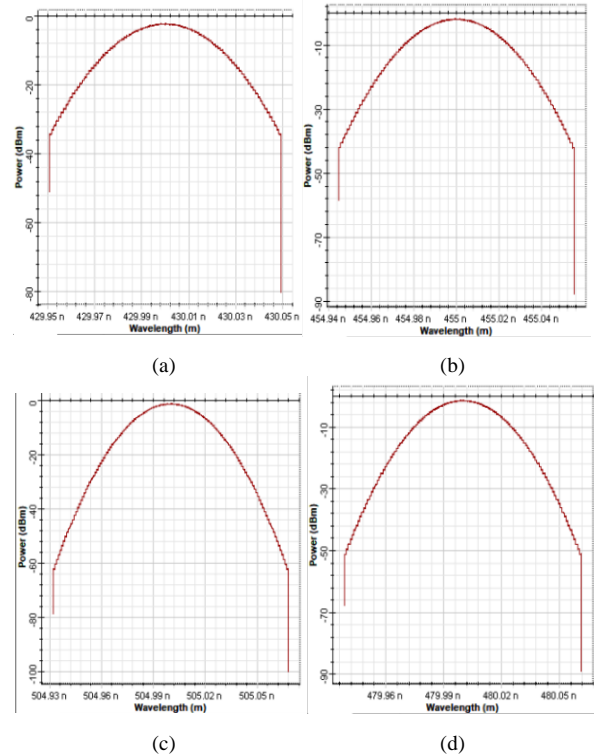


Figure 3. Optical Source Spectrum
(a) 430 nm, (b) 455 nm, (c) 480nm, and (d) 505 nm

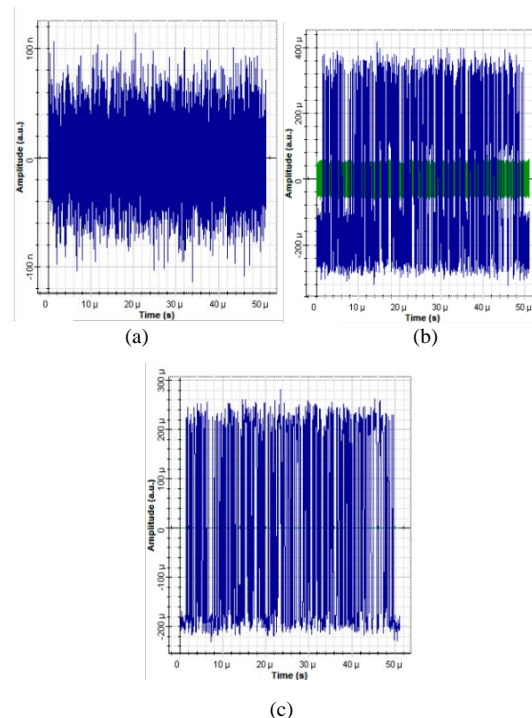


Figure 4 Electrical spectrum a) ambient short noise spectrum, b) after TIA-DC block, and c) after filtering (LPF)

O/E detection on the receiver side, where the output signal is observed on the ambient noise signal output as a representation of the noise in the demodulator device.

Based on Figure 4 (a), it can be seen that there is a noise that has a peak-to-peak power in the range of -100 nano-amplitude unit (a.u) to 100 (a.u). So to increase the power of the received signal, amplification by TIA, and bias by a DC block are required.

Figure 4 (b) shows that the signal output is still affected by noise (green signal spectrum) in the power range of -100 a.u to 100 a.u. So the gain and DC bias still need to be able to select the existing noise. This study places the LPF with a cut-off frequency of 0.75-bit rate to minimize noise power. The placement of the LPF has been able to reduce the noise power to within the range of 0 a.u, although the signal power has decreased from peak to peak -400μ to 400μ a.u to peak to peak -200μ to 200μ a.u as shown in Figure 4 (c).

3.2 Performance of Multiplexing 2x2 on Indoor Li-Fi System

Observation of the performance of this 2x2 mux system is based on the parameters Min. BER, Max Q-factor, and SNR are obtained due to the influence of bit rate variations and LOS distance for each channel.

Figure 5 shows that the increase in bit rate and distance has a significant effect on increasing the BER value. Suppose we refer to the ITU-T standard for threshold Min. BER optical communication 10^{-12} , the 2x2 mux system can meet the standard for operating bit rates of 10 Mbps to 30 Mbps per channel at a distance of 3 meters but is already below the standard at a bit rate of 40 Mbps. At a distance of 3 meters, the increase in BER values starts from 1.45×10^{-45} (channel 1) and 5.15×10^{-47} (channel 2) in the bit rate range of 10 Mbps up to 2.45×10^{-8} (channel 1) and 1.74×10^{-8} (channel 2) in the bit rate range of 40 Mbps.

Based on statistical data at a distance of 3 meters for all bit rate variations, the standard deviation of the graph of increasing the BER value for channel 1 (430 nm) is 1.225×10^{-8} , while for channel 2 (455 nm), it is 8.7×10^{-9} . However, with up to 4 meters of LOS distance, a 2x2 mux system can meet standards limited to a bit rate of 20 Mbps. The increase in the BER value at that distance has a standard deviation value of 2.589×10^{-7} for channel 1 and 2.101×10^{-7} for channel 2. Therefore, it can be analyzed that the value of Min. BER of channel 2 obtained is lower than that of channel 1.

Observations on the Max Q-factor values for channel 1 and channel 2 show that the increase in bit rate and distance also significantly affects the decrease in the Q-factor value, as shown in Figure 6.

As with the BER parameter, the 2x2 mux system can meet the standard for operating bit rates of 10 Mbps to 30 Mbps per channel at a distance of 3 meters but is already below the standard bit rate of 40 Mbps (threshold $Q = 7$).

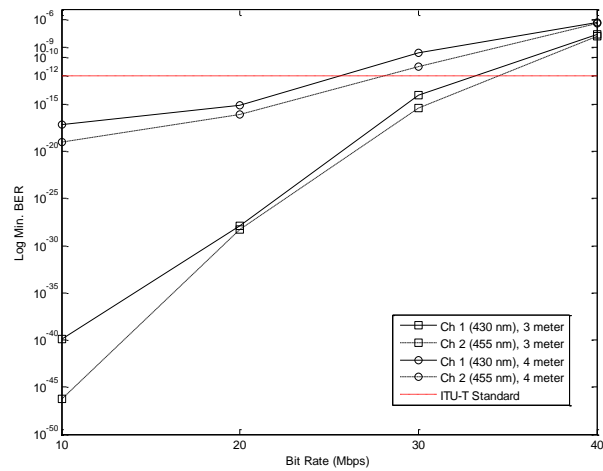


Figure 5 Min. BER for Mux 2x2

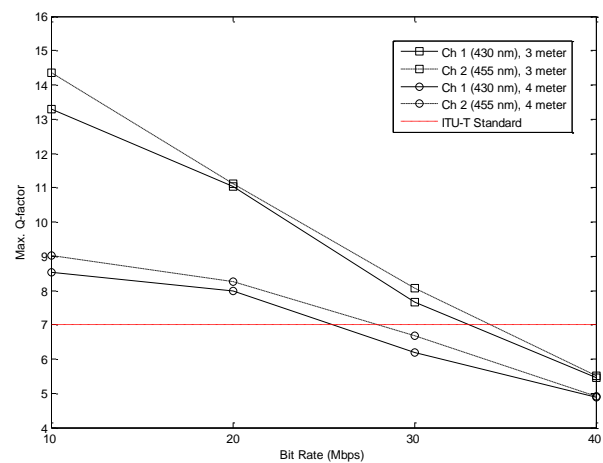


Figure 6 Max. Q-factor for Mux 2x2

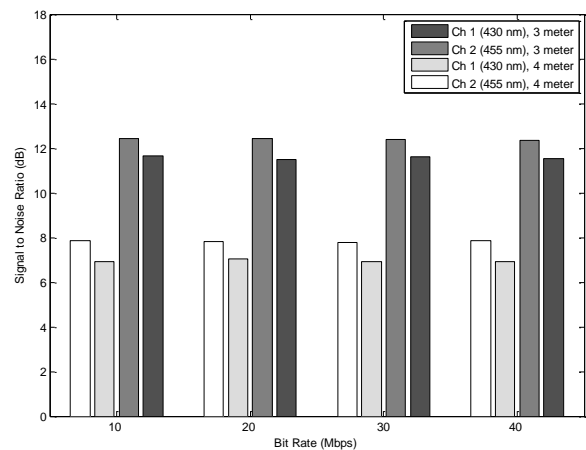


Figure 7 SNR for Mux 2x2

Meanwhile, for a distance of 4 meters, the mux 2x2 system only meets the standard of up to 20 Mbps. Besides that, the Q-factor value of channel 2 is higher than channel 1 for all variations of bit rate and distance. So, it can be analyzed from the Q-factor reduction curve from the bit rate range of 10 to 40 Mbps, which has a standard deviation of 3.482 for channel 1 and 3.824 for channel 2 at a distance of 3 meters. Meanwhile, the

standard deviation obtained at a distance of 4 meters is 1.675 for channel 1 and 1.814 for channel 2.

On the other hand, the decrease in SNR values for channel 1 and channel 2 as the LOS distance increases from 3 to 4 meters is 4.1 dB to 4.4 dB, as shown in Figure 7. However, the increase in bit rate from 10 Mbps to 40 Mbps is relatively minimal. So, it can be analyzed that the increase in bit rate has no significant effect on the SNR value, but it does affect the BER and Q-factor values. Therefore, there is an opportunity to develop this multiplexing model by increasing the quality of signal processing at the receiver so that it is reliable for a higher bit rate.

3.3 Performance of Multiplexing 4x4 on Indoor Li-Fi System

As is the case for the 2x2 mux system, the observation of the performance of the 4x4 mux system is analyzed based on the test results due to the influence of bit rate variations and LOS distance for four channels with channel spacing of 25 nm.

Based on Figure 8 shows that the increase in bit rate and distance has a significant effect on the increase in the BER value for all channels. Similar to the 2x2 mux system, the 4x4 mux system can meet the standard for all channels at an operating bit rate of 10 Mbps to 30 Mbps per channel at a distance of 3 meters but is below the ITU-T standard at a bit rate of 40 Mbps. Based on Figure 8, the curve for increasing the BER value at a distance of 3 meters obtained values ranging from 4.4×10^{-61} (channel 4), 1.07×10^{-52} (channel 3), 6.27×10^{-44} (channel 2), and 3.93×10^{-47} (channel 1) in the range of 10 Mbps bit rate. Based on these results indicate that the use of a longer wavelength (lower frequency) results in lower BER values, especially for channel 3 (480 nm) and channel 4 (505 nm). Even the increase in the curve for channel 4 can reach a standard deviation of 2.485×10^{-9} .

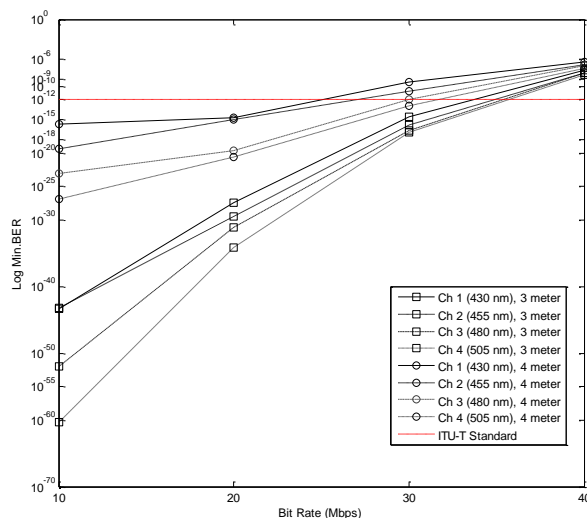


Figure 8 Min. BER for Mux 4x4

On the LOS distance of 4 meters, all channels can achieve a BER value above the standard up to a bit rate of 20 Mbps. The BER value of all channels appears from 1×10^{-28} to 1×10^{-17} (10 Mbps), a between 1×10^{-24} up to 1×10^{-13} (20 Mbps). At a bit rate of 30 Mbps and a distance of 4 meters, channels 3 and 4 comply with the BER value range of 10^{-10} . These results can be the reference for the wavelength utilization a 2x2 mux system, which can reach the standard by using channels 3 and 4. While modeling, the 4x4 mux system has yet to be able to meet the standard with an increase in the bit rate of 40 Mbps and a distance of 4 meters.

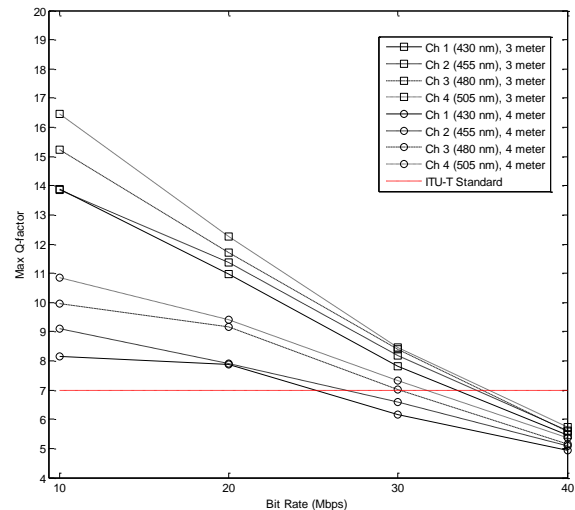


Figure 9 Max. Q-factor for Mux 4x4

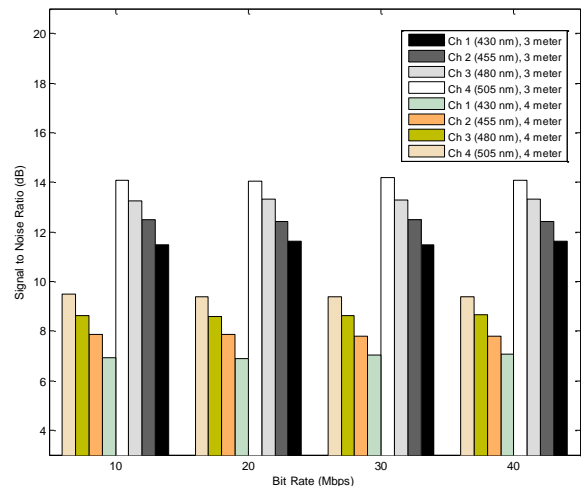


Figure 10 SNR for Mux 4x4

Observation on the Max Q-factor values for 4x4 mux system are also linear with BER results. The increase in bit rate and distance also significantly affects the decrease in Q-factor value, as shown in Figure 9. The 4x4 mux system can meet standards of up to 30 Mbps bit rate at a distance of 3 meters, whereas at a bit rate of 40 Mbps, no channel has a Q-factor value of more than 7. Furthermore, at a distance of 4 meters, the results obtained are that all channels are capable of above the standard up to a bit rate of 20 Mbps, but only

channel 3 and channel 4 meet the standard at a bit rate of 30 Mbps. On the other hand, the decrease in SNR values for channel 1 to channel 4 as the LOS distance increases from 3 to 4 meters is 4.3 dB to 4.5 dB, as shown in Figure 10. However, the increase in bit rate from 10 to 40 Mbps is relatively minimal. Therefore, the increase in the bit rate does not significantly affect the decrease in the value of SNR, so it is necessary to develop a multiplexing model or observation of responsivity and signal processing at the receiver so that it is reliable for a higher bit rate.

4. Conclusion

Based on the results, the increase in bit rate and distance significantly increases the BER value and decreases the Q-factor value. Both the 2x2 and 4x4 mux systems can meet standards up to a bit rate of 30 Mbps at a LOS distance of 3 meters, while at a bit rate of 40 Mbps, there are no channels that meet the ITU-T standard. In addition, the quality of the signal received at a distance of 4 meters, the 2x2 mux system can only reach the standard at a bit rate of 20 Mbps for all channels. However, channel 3 and channel 4 on the mux 4x4 system model still have a BER and Q-factor that meet the standard in the bit rate of 30 Mbps. However, the decrease in the SNR value affected by the bit rate increase and distance is insignificant. Therefore, it becomes an opportunity for further observation of the proposed multiplexing system, detection scheme, or responsivity, and signal processing on the receiver side to reliable on the higher bit rate.

Acknowledgment

This work is supported by the Photonic Laboratory of Institut Teknologi Telkom Purwokerto and the Smart System Laboratory of Universitas Gadjah Mada. The all authors thank LPPM of IT Telkom Purwokerto for the funding in this research.

Reference

- [1] V. Swetha and E. Annadevi, "SURVEY ON LIGHT-FIDELITY," in *International Conference on Smart Systems and Inventive Technology (ICSSIT 2018)*, 2018, no. Icassit, pp. 355–358.
- [2] M. Dehghani Soltani, A. A. Purwita, I. Tavakkolnia, H. Haas, and M. Safari, "Impact of Device Orientation on Error Performance of LiFi Systems," *IEEE Access*, vol. 7, no. c, pp. 41690–41701, 2019.
- [3] Tezcan Cogalan and Harald Haas and Li-Fi, "Why Would 5G Need Optical Wireless Communications?," *IEEE*, 2017.
- [4] F. Aftab, M. N. U. Khan, and S. Ali, "Light fidelity (Li-Fi) based indoor communication system," *Int. J. Comput. Networks Commun.*, vol. 8, no. 3, pp. 21–31, 2016.
- [5] L. E. M. Matheus, A. B. Vieira, L. F. M. Vieira, M. A. M. Vieira, and O. Gnawali, "Visible Light Communication: Concepts, Applications and Challenges," *IEEE Commun. Surv. Tutorials*, vol. 21, no. 4, pp. 3204–3237, 2019, doi: 10.1109/COMST.2019.2913348.
- [6] H. D. Huynh, K. Sandrasegaran, and S. C. Lam, "Modelling and Simulation of Handover in Light Fidelity (Li-Fi) Network," *IEEE Reg. 10 Annu. Int. Conf. Proceedings/TENCON*, vol. 2018-October, no. October, pp. 1307–1312, 2019, doi: 10.1109/TENCON.2018.8650221.
- [7] A. Yesilkaya, A. A. Purwita, E. Panayirci, H. V. Poor, and H. Haas, "Flexible LED Index Modulation for MIMO Optical Wireless Communications," *2020 IEEE Glob. Commun. Conf. GLOBECOM 2020 - Proc.*, 2020, doi: 10.1109/GLOBECOM42002.2020.9322528.
- [8] R. Riaz, S. S. Rizvi, F. Riaz, S. Shokat, and N. A. Mughal, "Designing of cell coverage in Light Fidelity," *Int. J. Adv. Comput. Sci. Appl.*, vol. 9, no. 3, pp. 44–53, 2018, doi: 10.14569/IJACSA.2018.090308.
- [9] H. B. Valiveti and B. A. Kumar, "Handoff strategies between wireless fidelity to light fidelity systems for improving video streaming in high-speed vehicular networks," *Int. J. Commun. Syst.*, vol. 34, no. 6, pp. 1–15, 2021, doi: 10.1002/dac.4285.
- [10] P. Kuppusamy, S. Muthuraj, and S. Gopinath, "Survey and challenges of Li-Fi with comparison of Wi-Fi," *Proc. 2016 IEEE Int. Conf. Wirel. Commun. Signal Process. Networking, WiSPNET 2016*, pp. 896–899, 2016, doi: 10.1109/WiSPNET.2016.7566262.
- [11] H. B. Eldeeb, S. M. Mana, V. Jungnickel, P. Hellwig, J. Hilt, and M. Uysal, "Distributed MIMO for Li-Fi: Channel Measurements, Ray Tracing and Throughput Analysis," *IEEE Photonics Technol. Lett.*, vol. 33, no. 16, pp. 916–919, 2021, doi: 10.1109/LPT.2021.3072254.
- [12] M. Sasi Chandra, S. Saleem, S. L. Harish, R. Baskar, and P. C. Kishoreraj, "Survey on Li-Fi technology and its applications," *Int. J. Pharm. Technol.*, vol. 8, no. 4, pp. 20116–20123, 2016.
- [13] C. Chen, I. Tavakkolnia, M. D. Soltani, M. Safari, and H. Haas, "Hybrid multiplexing in OFDM-based VLC systems," in *IEEE Wireless Communications and Networking Conference, WCNC*, May 2020, vol. 2020-May, doi: 10.1109/WCNC45663.2020.9120825.
- [14] Y. Tan and H. Haas, "Coherent LiFi System with Spatial Multiplexing," *IEEE Trans. Commun.*, vol. 69, no. 7, pp. 4632–4643, Jul. 2021, doi: 10.1109/TCOMM.2021.3074216.
- [15] C. P. Liu and A. J. Seeds, "Transmission of wireless MIMO-type signals over a single optical fiber without WDM," *IEEE Trans. Microw. Theory Tech.*, vol. 58, no. 11 PART 2, pp. 3094–3102, 2010, doi: 10.1109/TMTT.2010.2074510.
- [16] K. D. Salman and E. K. Hamza, "Visible Light Fidelity Technology: Survey," *Iraqi J. Comput. Commun. Control Syst. Eng.*, vol. 21, no. 2, pp. 1–15, 2021, doi: 10.33103/uo.ijccce.21.2.1.
- [17] S. Razzaq, N. Mubeen, and F. Qamar, "Design and Analysis of Light Fidelity Network for Indoor Wireless Connectivity," *IEEE Access*, vol. 9, pp. 145699–145709, 2021, doi: 10.1109/ACCESS.2021.3119361.
- [18] A. A. Purwita and H. Haas, "IQ-WDM for IEEE 802.11bb-based LiFi," in *IEEE Wireless Communications and Networking Conference, WCNC*, May 2020, vol. 2020-May, doi: 10.1109/WCNC45663.2020.9120567.
- [19] C. Chen, I. Tavakkolnia, M. D. Soltani, M. Safari, and H. Haas, "Hybrid multiplexing in OFDM-based VLC systems," *IEEE Wirel. Commun. Netw. Conf. WCNC*, vol. 2020-May, no. Vlc, 2020, doi: 10.1109/WCNC45663.2020.9120825.
- [20] R. ghahramani Negar Sendani, "Study the Effect of FOV in Visible Light Communication," *Int. Res. J. Eng. Technol.*, vol. 04, no. 10, pp. 759–763, 2017.
- [21] Optiwave, "OptiSystem Overview," *Optical Communication System Design Software*, 2022.